Electrocatalytic CO₂ hydrogenation to C₂ based products through C–C coupling over Cu(100) nanocube

Shyama Charan Mandal,[†] Biswarup Pathak,[†,*]

[†]Department of Chemistry, Indian Institute of Technology Indore, Indore 453552, India

*Email: biswarup@iiti.ac.in

Abstract

In this study, we have considered a Cu nanocube (Cu-NC) based catalyst exposed with (100) facets for CO_2 hydrogenation reactions. All the feasible mechanistic pathways for the formations of C_1 (HCOOH, CH_3OH and CH_4) and C_2 (C_2H_4 and C_2H_5OH) based products have been explored using the density functional theoretical calculations and the most plausible pathways have been identified. The calculated results are compared with the previous reports on the periodic Cu(100) and Cu(111) surfaces, and also on the surface of Cu_{85} nanocluster and Cu(111) monolayer. The in-depth mechanistic investigation shows that Cu-NC can be very selective towards the C_2 based products with a lower limiting potential (calculated) compared to the periodic surfaces. The underlying reasons for such findings have been explained and compared that with the periodic surfaces. We therefore, propose that the Cu-NC based catalysts can be more promising for C_2 based products.

KEYWORDS: Cu(100) nanocube, CO₂ hydrogenation, methanol, ethylene, ethanol, density functional theory

1. Introduction

Electrocatalytic CO_2 hydrogenation reaction can be a promising approach for renewable energy production through conversion of CO_2 to liquid fuel and such hydrogenation reactions are also very important for fundamental chemistry such as C-C coupling and C-H bond formation reactions.[1-3] Among various metals in heterogenous electrocatalytic CO_2 hydrogenation reaction, Cu has been found as an effective electrocatalyst for CO_2 hydrogenation reaction.[4] In the case of other electrodes, Ti, Fe, Ni, or Pt-based electrodes are found to be promising for hydrogen productions[5] whereas Ag, Au or Zn based electrodes are efficient for CO productions[6,7] and Pb, Pd, Au, Cd, In, Sn, or Ru-based electrodes favor formate[8-10] productions. Hori and co-workers have shown that CH_4 and C_2H_4 are the two major products on Cu based catalysts with high current density and Faradic efficiency (FE).[4,10,11] However, the required potential for CO_2 hydrogenation is relatively high (~1.0 V) and therefore, the efficiency of Cu based catalysts is less for such reaction.[12] Further to this, the selectivity of the product is less as various products can be achieved at comparable potential. Hence, the major difficulties in the electrochemical CO_2 hydrogenation reaction are high overpotential and low product selectivity which hamper the development and application of CO_2 hydrogenation reaction. Several research groups have reported that the selectivity and activity of CO_2 hydrogenation reaction are highly influenced by the morphology of the Cu surface. Hori and co-workers have demonstrated that CH_4 is the main product on Cu(111) surface whereas C_2H_4 is the major product on Cu(100) surface.[13-15] In this context, Koper and co-workers have shown two different pathways on the periodic Cu(100) surface for the formation of C_2 based product.[16-18] Both the pathways have some common intermediates which can form CH_4 at –0.8 to –0.9 V vs reversible hydrogen electrode (RHE). In this case, the most important step for C_2 based product formation is the dimerization of CO at ~-0.4 V vs RHE. After these reports,

Calle-Vallejo et al. have investigated the C_2 production mechanism using DFT calculations on periodic Cu(100) surface.[19] Nørskov and co-workers have also explored the CO_2 hydrogenation mechanism and shown that CO dimerization barriers on the periodic Cu(100) surface are less compared to that on the periodic Cu(111) surface.[20] Recently a detailed mechanistic pathways, required potentials, and various product selectivity have been investigated by Asthagiri and co-workers on periodic Cu(100) surface.[21] After this, Head-Gordon and co-workers have shown the mechanism of various C_2 based products on Cu(100) surface and compared with Cu(111) surface.[22] All of these reports show that the C−C bond formation step is favourable on the Cu(100) facet compared to that on the Cu(111) facet. Even if Cu based electrodes are a good choice for the development of CO_2 hydrogenation reaction, the high potential and selectivity still needs to be developed. In an effort to produce highly selective C_2 based products, Cu nanoparticles with (100) facets have been used in earlier studies.[23-25] In the case of nanoparticles, exposed (100) facet surface area is more compared to that on the periodic Cu(100) surface i.e., catalytic activity is more. Recently, Nilsson and co-workers have reported that Cu nanocube exposed with (100) facet shows more selectivity towards C_2 based product at a very low overpotential.[26] Their report shows that C_2H_4 can be formed at –0.60 V and CH_4 can be formed at –0.93 V vs. RHE. However, C_2 based product, C_2H_4 and C_2H_5OH is obtained along with some undesired H_2, $HCOO^-$, CH_3OH and CH_4 products. Even after several excellent experimental and theoretical reports, the underlying reason behind Cu surface structure and the selectivity of the product is still unknown. Specifically, the most favourable pathways of various products with their adsorption energy and reaction free energy are not fully understood. Therefore, finding out the most favourable mechanisms for all C_1 and C_2 based products are highly essential to get the idea about the product selectivity of any catalyst. Experimental mechanistic studies of CO_2 hydrogenation reaction are very challenging

3

due to the complexities of spectroscopic operation on the reactants and intermediates. Even if several experimentalists have shown via in situ IR spectroscopy and confirmed CO_2, CO, and formate are important intermediates, this cannot identify all the surface species during the reaction specially for two carbon atoms-based products.[27,28] Besides, Koper and co-workers have proposed a CO_2 hydrogenation mechanism, but it does not include all the possible pathways of CO_2 hydrogenation reaction.[16] Their study can identify only the stable intermediates and it is obtained after observing the product only. So, the theoretical free energy calculations of all the possible pathways are very promising in terms of identifying the reaction pathways. In an effort to this, Rossmeisl and co-workers have shown various important intermediates for alcohol formation.[29] Hence, it is highly essential to theoretically investigate the full mechanistic pathways due to the limitation in experimental studies. However, C_2H_4 and C_2H_5OH are highly useful C_2 based CO_2 hydrogenated product along with various C_1 based products (HCOOH, CH_3OH and CH_4).[30-34] For example, C_2H_4 is an important feedstock in chemical industries as C_2H_4 oligomerization can produce highly valuable ethylene oxide, polyethylene, and diesel. Besides, C_2H_5OH can be used as a chemical feedstock for C_2H_4, glycol ether, amines, and esters formation. Hence, the present study investigates the development of CO_2 hydrogenation reaction mechanistic pathways for the formation of C_1 as well as C_2 based products. For this, we have modelled a Cu nanocube (Cu-NC) exposed with Cu(100) facets (Figure 1), as such nanoparticles have been experimentally reported to be more efficient and selective catalyst compared to the periodic Cu(100) surface/facet for the C–C coupling and therefore formation of C_2 based products. As a part of the attempt, stability of the Cu-NC, adsorption energy of all the considered intermediates and reaction free energy of each elementary steps have been calculated. These adsorptions and reaction free energy information can give a quantitative idea of the Cu electrode for CO_2 hydrogenation reaction based on the surface

morphology, and which can guide the future direction of modelling efficient catalyst. Shortly, in this work, we have computationally investigated the most plausible pathways of C_1 and C_2 based CO_2 hydrogenated products (such as CH_3OH, $HCOOH$, CH_4, C_2H_4 and C_2H_5OH) on the Cu-NC and found out the factors responsible for favoring those reaction pathways.
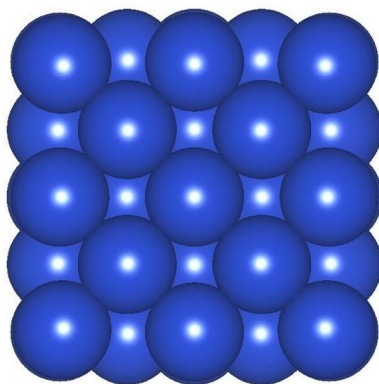

Figure 1: Modelled Cu nanocube (Cu-NC) exposed with Cu(100) surface for CO_2 hydrogenation reaction.

2. Computational Details

All the first principles calculations have been performed using the projector augmented wave (PAW) method as employed in the Vienna Ab initio Simulation Package (VASP).[35-37] The description of the exchange-correlation interaction in the calculation has been incorporated with the generalized gradient approximation (GGA) of Perdew–Burke–Ernzerhof (PBE) functional.[38-40] The Grimme's D3 semiempirical dispersion energy corrections have also been included in our calculations to account the corrections for the non-covalent interactions.[41] More than 15 Å vacuum space has been considered in all the three directions to avoid any periodic interactions. The plane-wave basis cutoff energy has been set to 470 eV. Here all the structures were optimized until the

energy convergence criteria becomes less than that of 1×10^{-4} eV and forces become less than 0.02 eV/Å. Moreover, we have calculated the total energies of the Cu NC using a series of k-points ($1\times1\times1$, $3\times3\times3$ and $5\times5\times5$ gamma centered k-points grid) and it has been observed a little improvement of 9.2×10^{-4} and 7.1×10^{-4} eV in the total energy using $3\times3\times3$ and $5\times5\times5$ gamma centered k-points, respectively compared to $1\times1\times1$ gamma centered k-points. Hence, all the calculations have been performed using $1\times1\times1$ gamma centered k-points. We have calculated adsorption energies of all the considered CO_2 hydrogenation intermediates using the following equation (1):

$$E_{ad} = E_{NC+adsorbate} - (E_{adsorbate} + E_{NC})\qquad(1)$$

In the above equation (1), E_{ad} is the adsorption energy of any intermediate, $E_{NC+adsorbate}$ is the total energy of the optimized NC with adsorbate whereas $E_{adsorbate}$ and E_{NC} are the single point energies of adsorbate and Cu-NC (within the optimized geometry of NC+adsorbate) respectively. In the case of the H atom energy, we have used the computational hydrogen electrode (CHE) model concept as reported by Nørskov and co-workers.[42] Moreover, for the calculation of reaction free energy of each elementary steps we have used the following equation (2):

$$\Delta G = \Delta E + \Delta ZPE - T\Delta S\qquad(2)$$

In the above equation (2), ΔG is the reaction free energy of the considered particular elementary step, ΔE is the total energy difference of the final and initial states of the considered step, ΔZPE is the change in zero-point energy, ΔS is the change in entropy of the considered step and T is the temperature. The zero-point energy has been calculated using $\sum\frac{1}{2}h\upsilon_i$ where h is the Planck's constant and υ_i is the vibrational frequency. Here, we have neglected the entropy term during the reaction free energy calculation of each elementary step. During an external applied potential (U),

the chemical potential of each step shifts by eU where e is the electronic charge transferred in each elementary step.[43,44] Moreover, we have checked transition states and calculated the energy barriers for some of the important steps using the nudged elastic band (CI-NEB, six climbing-image) and dimer methods.[45,46] In this case we have not considered the effect of pH as reversible hydrogen electrode (RHE) is considered as 0 V at all pH values.[44] A set of $3\times3\times3$ k-point grid has been used for some of the important intermediates to investigate the electronic structure of the intermediates. We have also characterized all the intermediates by examining the absence of vibrational frequency. Besides, the Bader atomic charges of some of the important intermediates have been calculated using the Henkelman code with the near-grid algorithm refine-edge method.[47-49] The adsorbed intermediates have been represented by an asterisk sign (*) throughout the manuscript.

3. Results and discussion

In this section, we have discussed the Cu-NC stability using energetic, dynamic, and thermal stability analysis. After stability analysis, we have considered the stable form of the Cu-NC for the investigation of CO_2 hydrogenation reaction catalytic activity based on the adsorption energy of each considered intermediates and reaction free energy of every elementary step for C_1 and C_2 based product formation.

3.1. Stability analysis

The stability of the considered Cu-NC has been examined through various approaches. At first, we have investigated the energetic stability by calculating the formation and cohesive energies of the

Cu-NC to check the stability of the considered structure with respect to the bulk Cu structure. We have used equation 4 and equation 5 for the calculation of cohesive energy (E_{coh}) and formation energy (E_{for}) of the considered Cu-NC respectively.[50,51]

$$E_{coh} = E_{Cu\text{-}NC}/N - E_{Cu} \qquad (4)$$

$$E_{for} = E_{Cu\text{-}NC}/N - \mu_{Cu} \qquad (5)$$

In the above equations, $E_{Cu\text{-}NC}$, E_{Cu}, μ_{Cu}, and N are the total energy of the Cu-NC, energy of an isolated Cu atom, chemical potential of a Cu atom and total number of atoms present in the Cu-NC, respectively. For comparisons, we have also calculated the formation energy and cohesive energy of the periodic Cu(100) and Cu(111) surface and then compared with the available experimental values. Our calculated formation and cohesive energy values are tabulated in Table 1. The calculated formation and cohesive energy values for periodic Cu(111) surface are in agreement with the experimental formation and cohesive energy values on periodic Cu(111) surface.[52] Hence, the considered level of theory is acceptable for further study. Further to this, we have checked the dynamic stability of the Cu-NC using density functional perturbation theory which is implemented in VASP. Our calculated, dynamic stability analysis shows imaginary frequency in the order of ~ 40i cm^{-1}. Several earlier reports have shown that the systems can be considered as stable if the imaginary frequency is below 35i cm^{-1}.[53,54] Therefore, the considered Cu-NC is dynamically unstable structure i.e., Cu-NC has a possibility of interconversion to other form. Even though our considered approach is electrochemical there will be some nonelectrochemical steps which can be performed at experimental thermal condition. In general, thermal CO_2 hydrogenation reaction is performed at 473−573 K temperature.[55] So, it is highly important to check the stability of the considered Cu-NC at that temperature range for the operation of the reaction. To investigate these aspects, we have investigated the thermal stability of Cu-NC

8

at 300, 400 and 500 K (Figure 2a) using ab initio molecular dynamics (AIMD) simulations with Nose´ thermostat model and NVT ensemble with a time step of 1 femtosecond (fs) for 20 picoseconds (ps).[56] We find that there is no significance change in the energy as well as structure throughout the simulation of the Cu-NC at 300 K. However, we have noticed fluctuation in energy at 400 K after 13 ps. The same has been observed at 500 K after 10 ps. Therefore, we have checked the structure of the Cu-NC after the completion of the simulation at 400 and 500 K. All the structures obtained after completion of the AIMD simulation have been shown in Figure S1. We have found a significant change in the Cu-NC structure after completion of the AIMD simulation at 400 and 500 K. The Cu-NC is now converted into another geometry, where the structure looks like an octahedral structure (Figure 2b). Therefore, there is a chance of interconversion of the Cu-NC during the operation of the CO_2 hydrogenation reaction. Hence, we have considered the distorted Cu-NC (Cu-dNC) and checked its stability using energetic, dynamic, and thermal stability analysis.

Table 1: Formation and cohesive energies of Cu-NC, Cu-dNC, periodic Cu(100) and Cu(111) surface. The experimental formation and cohesive energy values for the periodic Cu(111) surface are given in parenthesis for comparisons.[52]

Cu-NC and periodic systems	Formation energy (eV/atom)	Cohesive energy (eV/atom)
Cu-NC	1.03	-2.96
Cu-dNC	0.99	-3.01
periodic Cu(100) surface	0.46	-3.54
periodic Cu(111) surface	0.26 (0.31)[52]	-3.85 (-3.49)[52]

Our calculated cohesive and formation energy values indicated that the simulated Cu-dNC is more stable than the Cu-NC. Furthermore, we have checked the dynamic stability of Cu-dNC using

phonon calculation as implemented in VASP. Our study shows very small imaginary frequency up to 10i cm^{-1}. Hence, the Cu-dNC structure is dynamically more stable compared to the Cu-NC structure. After confirmation of energetic and dynamic stability of the Cu-dNC, we have examined the thermal stability of the Cu-dNC at 300, 500 and 700 K for 20 ps with a time step of 1 fs (Figure 2b). All the structures obtained after completion of the AIMD simulation of Cu-dNC have been shown in Figure S2. Our AIMD simulations show there are no significant change in the energy as well as structure throughout the calculation at 300 K. The overall energy fluctuation is also less even at 500 and 700 K. Hence, the interconversion possibility to other local minimum energy structure of the Cu-dNC during the reaction is not expected in the 300 to 700 K temperature range. So, we can say Cu-dNC is a stable structure and therefore considered as a model catalyst for the CO_2 hydrogenation reaction.
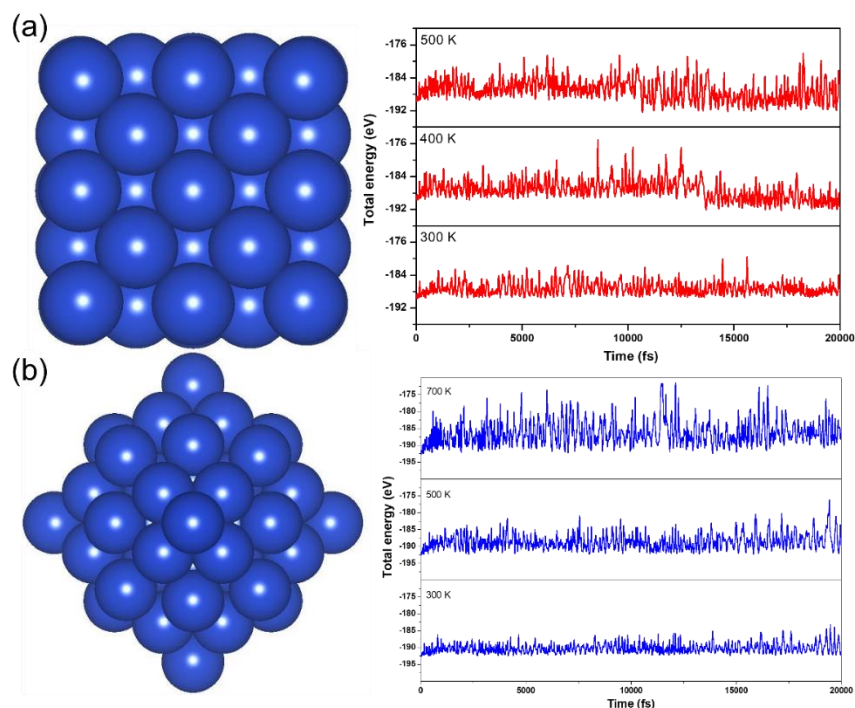

10

Figure 2: (a) Optimized structures of the Cu-NC and ab initio molecular dynamics (AIMD) simulations of Cu NC at 300, 400 and 500 K. (b) Optimized structures of the Cu-dNC and AIMD simulations of Cu-dNC at 300, 500 and 700 K.

3.2. Adsorption of different intermediates

Here, we have checked the applicability of Cu-dNC for CO_2 hydrogenation reaction in detail. At first, all the possible intermediates are identified, which can be formed during the CO_2 hydrogenation for the formation of C_1 (HCOOH, CH_3OH and CH_4) and C_2 based products (C_2H_4 and C_2H_5OH). All the possible adsorption sites on the Cu-dNC have been identified for all the considered intermediates as shown in Figure 3. There are four top, four bridge and three possible hollow sites on the Cu-dNC surface. Therefore, all these adsorption sites have been taken into consideration for the adsorption energy calculations of the intermediates. The preferred adsorption sites and adsorption energies are listed in Table 2 whereas the respective geometries for C_1, H, O and H_2O intermediates are shown in Figure S3 and the respective geometries for C_2 based intermediates are shown in Figure S4.
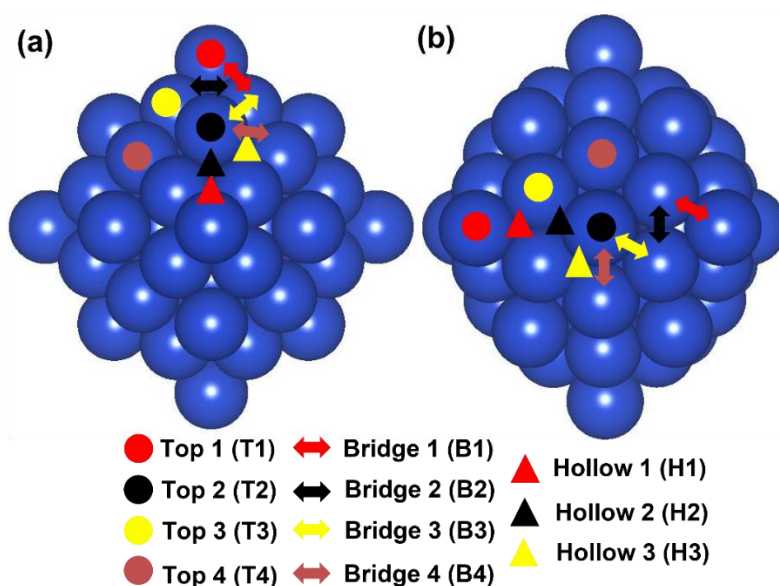
Figure 3: (a) Side and (b) top views of the considered Cu-dNC with all possible adsorption sites.

The calculated adsorption energies of most of the C_1 based intermediates are higher on the Cu-dNC surface compared to that on the periodic Cu(111) surface.[57] However, CO_2 interacts very weakly with an adsorption energy of -0.19 eV on the Cu-dNC surface. The same has been observed in several experimental and theoretical studies.[57-59] The *COOH intermediate also binds weakly on whereas *HCOO binds strongly on the catalytic surface. This may be due to the presence of two strong Cu–O bonds in case of *HCOO whereas in case of *COOH one Cu–C bond is present along with one Cu–O bond. Furthermore, to understand the reason behind the trends of adsorption energy, we have checked the projected density of states (PDOS) for *COOH and *HCOO. From Figure 4a-b, it is clear that the overlap among Cu-d orbitals and C+O-p orbital is less compared to the overlap among Cu-d orbitals and 2O-p orbital. Moreover, our calculated Bader atomic charges show that 0.29 |e| and 0.25 |e| charges are transferred from the Cu surface to the two O atoms of *HCOO, respectively whereas 0.26 |e| and 0.12 |e| charges are transferred from the Cu surface to the O and C-atom of *COOH. So, the amount of charge transfer is more for *HCOO compared to that for *COOH. Hence, adsorption energy is more in case of *HCOO on Cu-dNC compared to that for the *COOH. Another two important intermediates of CO_2 hydrogenation to C_1 based product formation are *HCO and *COH. In general, *HCO and *COH are two crucial intermediates for the selective C_1 based product formation of CH_3OH and CH_4, respectively.[57,60-62] Our calculated results show that *HCO binds weakly on the catalytic surface compared to the *COH. The calculated Bader atomic charges show that 0.13 |e| charges are transferred from the Cu surface to the C atom of *HCO whereas 0.15 |e| charges are transferred from the Cu surface to the C-atom of *COH. So, the amount of charge transfer is more for *COH compared to the *HCO from Cu-dNC i.e., adsorption energy is more for *COH compared to the *HCO. Besides, the

12

*H_2CO binds strongly on the catalytic surface compared to the periodic Cu(111) surface[57] i.e., the *H_2CO can be hydrogenated further for CH_3OH formation rather than desorption from the catalytic surface.

Table 2: Preferred adsorption sites and the adsorption energies of all the CO_2 hydrogenation related intermediates on the Cu-dNC.

C_1 based, H, O and H_2O intermediates		C_2 based intermediates	
Intermediates	Adsorption energy on Cu-dNC (eV)	Intermediates	Adsorption energy on Cu-dNC (eV)
*CO_2 (T2)	-0.19	*HCO-HCO (B3)	-2.35
*COOH (B3)	-2.84	*HCO-HCOH (B3)	-2.59
*HCOO (B1)	-4.09	*HCO-CO (B3)	-3.14
*HCOOH (T1)	-1.04	*COH-CO (B1)	-3.67
*CO (T2)	-1.28	*C-CO (B4)	-5.40
*HCO (T1)	-1.96	*C_2H_4 (T2)	-1.19
*COH (B4)	-3.71	*HC-CO (B3)	-3.55
*H_2COOH (B3)	-3.53	*H_2C-CO (B3)	-3.15
*H_2CO (B1)	-1.94	*HC-HCO (H3)	-4.99
*HCOH (B1)	-2.72	*H_2C-HCO (H2)	-3.20
*H_2COH (B1)	-2.37	*H_2C-H_2CO (B1)	-4.64
*H_3CO (H3)	-3.12	*HC-COH (H3)	-5.78
*H_3COH (T2)	-0.76	*C-HC (H3)	-4.81
*C (B4)	-6.24	*C-H_2C (B4)	-3.95
*CH (B4)	-6.02	*HC-HC (H3)	-4.85
*CH_2 (H3)	-4.21	*HC-H_2C (B3)	-3.26
*CH_3 (T1)	-2.38	*H_2C-HCOH (T2)	-1.16
*CH_4 (T2)	-0.25	*H_3C-HCO (B4)	-0.95
*H (H3)	-2.70	*H_3C-H_2CO (H3)	-3.19
*O (H3)	-5.60	*H_3C-HCOH (T1)	-2.41
*H_2O (T4)	-0.44	*H_3C-H_2COH (T3)	-0.77

In case of C_2 based products, intermediates adsorption energies are more compared to the adsorption energies of C_1 based intermediates. However, *HC-HCO adsorption energy is more compared to the *H_2C-CO adsorption energy as one extra strong Cu–O bond (1.936 Å) is present in case of *HC-HCO (Figure S4). The same has been observed in case of *H_2C-H_2CO (Cu–O bond

length is 1.843 Å) where adsorption energy is 3.48 and 3.69 eV high compared to the *H_2C-HCOH and *H_3C-HCO adsorption energy, respectively. Moreover, the adsorption energy of *H_3C-H_2CO is 0.78 eV more compared to the adsorption energy of *H_3C-HCOH. In this case also higher adsorption energy is due to the O binding with the active surface.

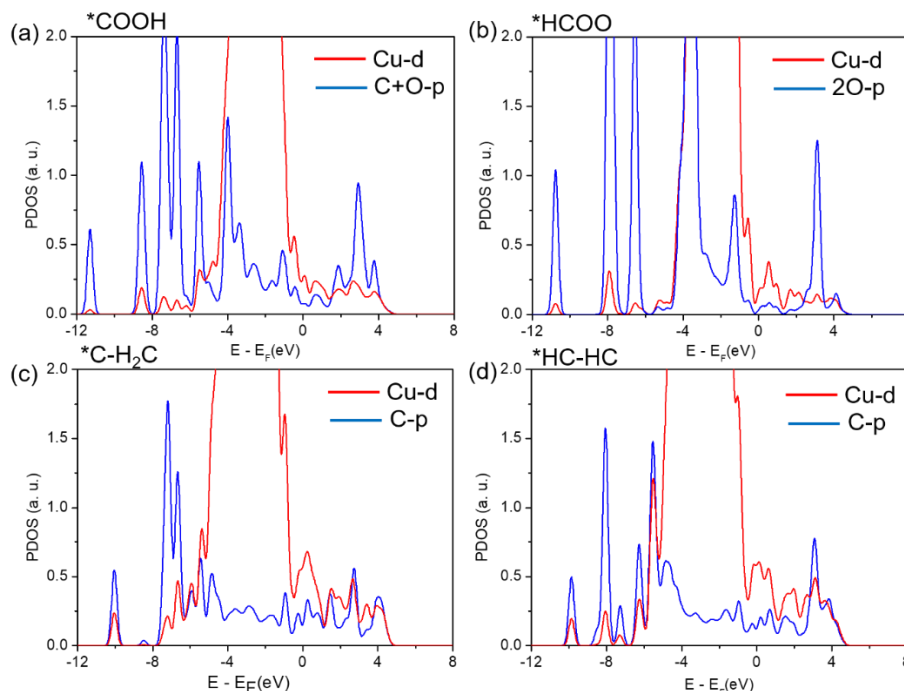**Figure 4**: Projected density of states plot of (a) *COOH, (b) *HCOO, (c) *C-H_2C, and (d) *HC-HC intermediates on Cu-dNC.

On the other hand, the adsorption energy of *HC-HC is 0.90 eV higher than that of *C-H_2C. This may be due to the presence of two single Cu-C in *HC-HC. To understand the reason behind the trends of adsorption energy we have checked the PDOS for *C-H_2C and *HC-HC. From Figure 4c and 4d it is clear that the overlap between Cu-d orbitals with C-p orbital is less for *C-H_2C compared to the overlap between Cu-d orbitals with C-p orbital of *HC-HC. Hence, adsorption energy is more in case of *HC-HC on Cu-dNC compared to that for *C-H_2C. Further to this, we

have noticed that presence of adsorbate on the catalytic surface does not distort the catalyst. Therefore, the nano catalyst is stable even in the presence of adsorbates.

3.3. CO_2 hydrogenation to C_1 based product formation

In this section, we have considered all the possible mechanistic pathways for C_1 based product formation from CO_2 and identified the most plausible pathways along with the potential determining steps (PDS) responsible for such reaction on the Cu-dNC. All the considered mechanistic pathways for the CO_2 hydrogenation to HCOOH, CH_3OH and CH_4 along with the calculated reaction free energies associated for each of those mechanistic steps are shown in Scheme 1.

3.3.1. Formation of HCOOH: Several earlier studies have confirmed that HCOOH is a common CO_2 hydrogenated product. Hence, we have started our discussion of mechanistic investigation from CO_2 to HCOOH. The adsorption energy analysis shows that CO_2 interacts weakly with the Cu-dNC surface. However, the calculated reaction free energy value shows that the CO_2 adsorption process is exergonic by 0.22 eV. Our earlier report has also shown that the reaction free energy of CO_2 adsorption step is exergonic on ZnO and Cu dopped ZnO based nanocages.[61] In the presence of H, one of the C=O bonds of *CO_2 can be weakened due to the hydrogenation at the C-center for the formation of *HCOO. Moreover, the *HCOO intermediate can be hydrogenated further at the O-center of *HCOO for the production of *HCOOH. Lastly, the HCOOH can be removed from the catalytic surface and the removal of HCOOH is 0.95 eV endergonic in nature. So, a massive input of energy is required for the of separation of HCOOH from the catalytic surface.

The formation of *HCOOH from *HCOO is calculated to be the potential rate determining step with a reaction free energy of 0.55 eV and the most favourable pathway for CO_2 hydrogenation to HCOOH on the Cu-dNC is $* + CO_2 \rightarrow *CO_2 \rightarrow *HCOO \rightarrow *HCOOH \rightarrow * + HCOOH$.
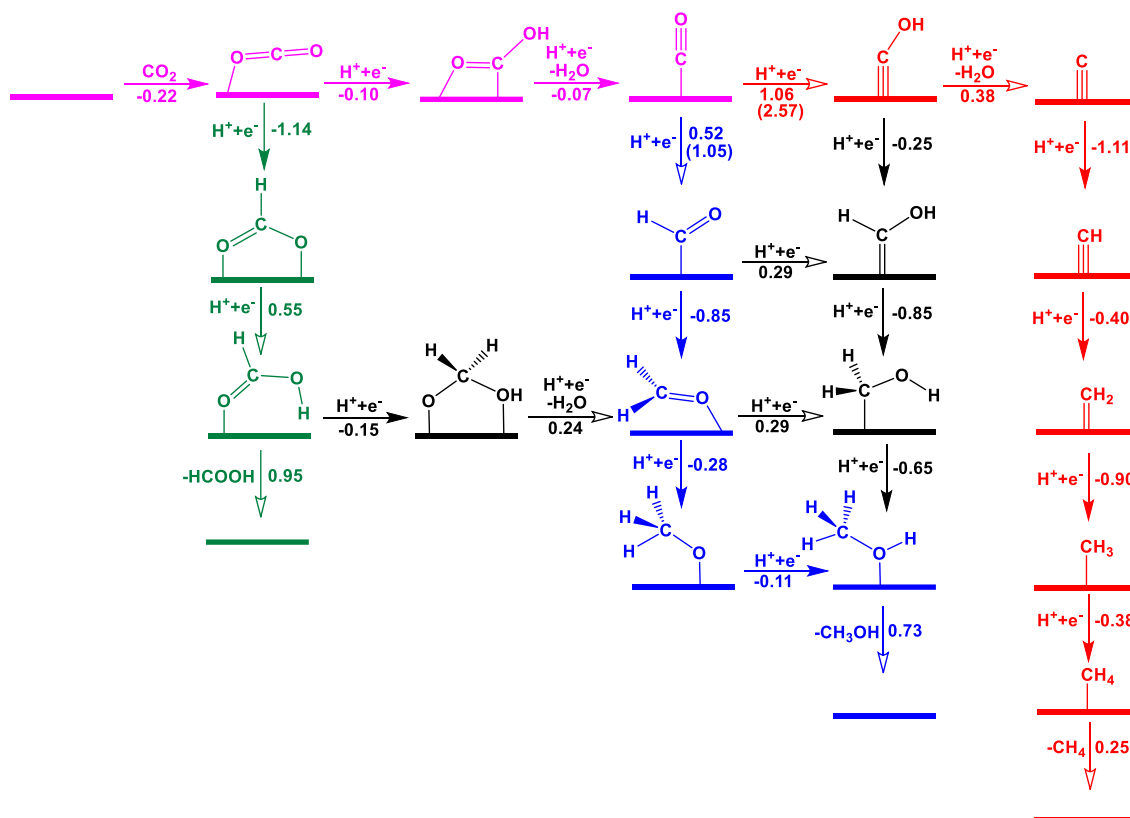
Scheme 1: All the possible mechanistic pathways with reaction free energies (in eV) for CO_2 hydrogenation reaction to HCOOH, CH_3OH and CH_4 on Cu-dNC. The values given in the parenthesis are the activation barriers in eV at 0 V vs. RHE. The common intermediates of most favourable pathways are highlighted in magenta color and the intermediates determine the selectivity of HCOOH, CH_3OH and CH_4 are highlighted in green, blue and red colors, respectively. The solid and hollow arrow heads represent the exergonic and endergonic steps, respectively.

3.3.2. Formation of CH_3OH: The CH_3OH is another important C_1 based CO_2 hydrogenated product. In this context several experimental studies have reported that *CO is an essential

16

intermediate for the formation of CH_3OH.[27,28] The adsorbed $*CO_2$ can be hydrogenated at the O-center for the formation of $*CO$. Our calculated results demonstrate that the formation of $*CO$ ($*COOH \rightarrow *CO$) is calculated to be very much reversible with a reaction free energy of 0.07 eV. Subsequently, $*CO$ can be hydrogenated for the formation of $*HCO/*COH$. Previous reports have shown that the $*HCO$ is responsible for CH_3OH formation whereas $*COH$ is responsible for CH_4.[57,61-63] Therefore, the product selectivity is very much dependent on the $*CO$ hydrogenation step. Scheme 1 shows that $*HCO$ formation is 0.54 eV more favourable compared to the formation of $*COH$. Moreover, our calculated activation barriers also shows that CH_3OH formation will proceeds via $*HCO$ intermediate. Hence, we can conclude that CH_3OH formation is more favourable compared to CH_4 formation on the Cu-dNC. We have also found out that $*HCO$ formation is 0.10 eV more favourable on Cu-dNC compared to the $*HCO$ formation on the periodic Cu(100) surface as reported by Asthagiri and co-workers using the same level of theory.[21] Besides, $*COH$ formation is 0.32 eV is more favourable on the periodic Cu(100) surface compared to that on the Cu-dNC as reported by Asthagiri and co-workers.[21] All these results indicate that Cu-dNC can be more selective towards CH_3OH formation compared to the periodic Cu(100) surface. In the next step, $*HCO$ can be hydrogenated for the formation of $*H_2CO/*HCOH$. Besides, $*H_2CO/*HCOH$ can be produced via other pathways as shown in scheme 1. The calculated results show that the formation of $*H_2CO$ is 1.14 eV more favourable compared to the formation of $*HCOH$. Subsequently, $*H_2CO$ can be hydrogenated to $*H_3CO/*H_2COH$ whereas $*HCOH$ can be hydrogenated to $*H_2COH$. The $*H_3CO$ formation is exergonic whereas $*H_2COH$ formation is endergonic from $*H_2CO$ i.e., the reaction will proceed via $*H_3CO$. Further to this, $*H_3CO$ and $*H_2COH$ can be hydrogenated for the formation of $*CH_3OH$. Eventually, CH_3OH can be separated, and the calculated results show that the removal of CH_3OH requires an amount of

0.73 eV energy. Considering all the above pathways and the most favourable CO_2 hydrogenation to CH_3OH pathway is * + CO_2 → *CO_2 → *COOH → *CO → *HCO → *H_2CO → *H_3CO → *H_3COH → * + CH_3OH, where the formation of the *CO → *HCO is the PDS with a reaction free energy of 0.52 eV. The previous reports on various Cu based surfaces [Cu(100) surface,[21] Cu_{85} nanocluster,[57] periodic Cu(111) surface[63] and Cu(111) monolayer[62]] have also reported that *CO → *HCO is the PDS for CO_2 hydrogenation to CH_3OH reaction. However, the calculated reaction free energy value of the PDS indicates that Cu-dNC can be used as an active catalyst compared to the periodic Cu(100), Cu(111) surface and Cu_{85} nanocluster for CH_3OH formation.[21,57,63]

3.3.3. Formation of CH_4:

3.3.3. Formation of CH_4: Along with HCOOH and CH_3OH, we have also investigated the mechanistic pathways of CO_2 hydrogenation to CH_4 formation via *COH intermediate. Here, *COH can be hydrogenated at the O-center followed by removal of H_2O and produce *C. Subsequent hydrogenations of *C would lead to the formation of *HC, *H_2C, *H_3C and *H_4C. Our calculated reaction free energy values indicate that all these subsequent hydrogenation steps are exergonic. In the final step, CH_4 can be separated from the catalytic surface of Cu-dNC with a reaction free energy of 0.25 eV. The *CO → *COH is the PDS for CO_2 hydrogenation to CH_4 with a reaction free energy of 1.06 eV. Hence the selectivity towards CH_4 formation would be less on the Cu-dNC. Earlier reports have shown that the reaction free energy of *CO → *COH step is 0.74, 1.11 and 0.71 eV on the periodic Cu(100) surface,[21] Cu(111) monolayer[62] and Cu_{85} nanocluster,[57] respectively. Hence, formation of CH_4 is highly unfavourable on the Cu-dNC compared to the periodic Cu(111) surface and Cu_{85} nanocluster and therefore, Cu-dNC can be highly selective towards CH_3OH formation compared to the CH_4 formation.

3.4. CO$_2$ hydrogenation to C$_2$ based product formation

Here we have considered all the possible mechanistic pathways for C$_2$ based products formation from CO$_2$ and identified the most plausible pathways with minimum applied potential on the Cu-dNC. It has been revealed in the previous section that at first CO$_2$ is converted to CO and several studies have shown that by CO$_2$ hydrogenation to C$_2$ based products formation proceeds via CO.[17,64] Hence, we have considered all the mechanistic pathways from *CO as shown in Scheme 2.

3.4.1. Formation of C$_2$H$_4$: The C$_2$H$_4$ is the simplest and highly useful C$_2$ based hydrocarbon which can be obtained from CO$_2$. Various mechanistic pathways have been investigated via *HCO and *COH pathways as illustrated in Scheme 2. As shown in scheme 2, *CO can be hydrogenated to *HCO and *COH and can be dimerized to form C$_2$ based intermediates. There can be various nonelectrochemical steps to obtain C$_2$ based intermediates like *COH-CO, *HCO-HCO, *HCO-CO and *CO-CO. We have not discussed the *CO dimerization step as we could not able to optimize the *CO-CO intermediate on the Cu-dNC catalytic surface. Most of these nonelectrochemical dimerization steps are exergonic whereas the formation of *COH-CO formation is calculated to be more or less reversible and the *HCO-CO formation is endergonic. Our calculated activation barriers also reveal that dimerization of *HCO to *HCO-HCO is 1.61 eV more favourable compard to the *HCO-CO formation. Recently, Wang and co-workers have shown that the *HCO dimerization step is exergonic on the Cu(111) and F–Cu(111) facets.[65] The same has been observed by Asthagiri and co-workers on the periodic Cu(100) surface.[21] Hence, the CO$_2$ hydrogenation to C$_2$ based product may mainly proceed via *HCO-HCO intermediates. After the nonelectrochemical dimerization steps, subsequent proton transfer leads to the formation of various intermediates like *C-CO from *COH-CO, *HCO-HCO from *HCO-CO and *HCO-

HCOH from *HCO-HCO. All of these proton transfer steps are exergonic in nature. Subsequently, *HCO-HCOH can be hydrogenated at the OH-center for the formation of *HC-HCO. Subsequent hydrogenation at the CH-center of the *HC-HCO leads to the formation of *H_2C-HCO with a reaction free energy of -0.44 eV. Then, *H_2C-HCO can form *H_2C-HCOH which is also an exergonic step. The successive hydrogenation and removal of water will form *HC-H_2C which can be a reversible step (0.02 eV). The further hydrogenation of *HC-H_2C would lead to the formation of *C_2H_4. Moreover, we have investigated the further hydrogenation of *C-CO even though this pathway is unfavourable. The subsequent hydrogenation of *C-CO would result in the formation of *C_2H_4 via *HC-CO, *HC-COH, *C-HC, *C-H_2C/*HC-HC and *HC-H_2C intermediates. We have also identified the *C_2H_4 formation pathway via nonelectrochemical *H_2C dimerization step. Ultimately, C_2H_4 can be removed from the surface for the regeneration of the catalyst. This step requires an amount of 1.08 eV energy. Among all the probable pathways, the most favourable pathway for CO_2 hydrogenation to C_2H_4 is * + CO_2 → *CO_2 → *COOH → *CO → *HCO → *HCO-HCO → *HCO-HCOH → *HC-HCO → *H_2C-HCO → *H_2C-HCOH → *HC-H_2C → *C_2H_4 → * + C_2H_4 with a rection total free energy of -1.02 eV. Hence, CO_2 hydrogenation to C_2H_4 is thermodynamically favourable. Nørskov and co-workers have also shown that C_2H_4 pathways proceeds via *CHO and *HCO-HCO intermediates at -0.74 V.[44] Moreover, our investigated route for C_2H_4 formation is similar as reported by Asthagiri and co-workers on the periodic Cu(100) surface.[21] Conversely, the most favourable pathway is different from Head-Gordon's report as they have shown *COCHO formation is exergonic for C_2 based products formation.[22] Moreover, our calculated results show that *CO → *HCO is the PDS for C_2H_4 formation with a reaction free energy of 0.52 eV. Besides, the *CO → *HCO, *H_2C-HCOH → *HC-H_2C, *HC-H_2C → *C_2H_4 and *C_2H_4 → * + C_2H_4 steps are endergonic which can be

downhill at applied potential of -0.52 V. Asthagiri and co-workers have also shown that the *CO → *HCO step is most endergonic step with a reaction free energy of 0.62 eV on the periodic Cu(100) surface for C_2H_4 formation.[21] Along with this, Nilsson and co-workers have reported that CO_2 can be converted to C_2H_4 at -0.60 V on the Cu cube.[26] Hence, formation of C_2H_4 is highly favourable on the Cu-dNC compared to that on the periodic Cu(100) surface.
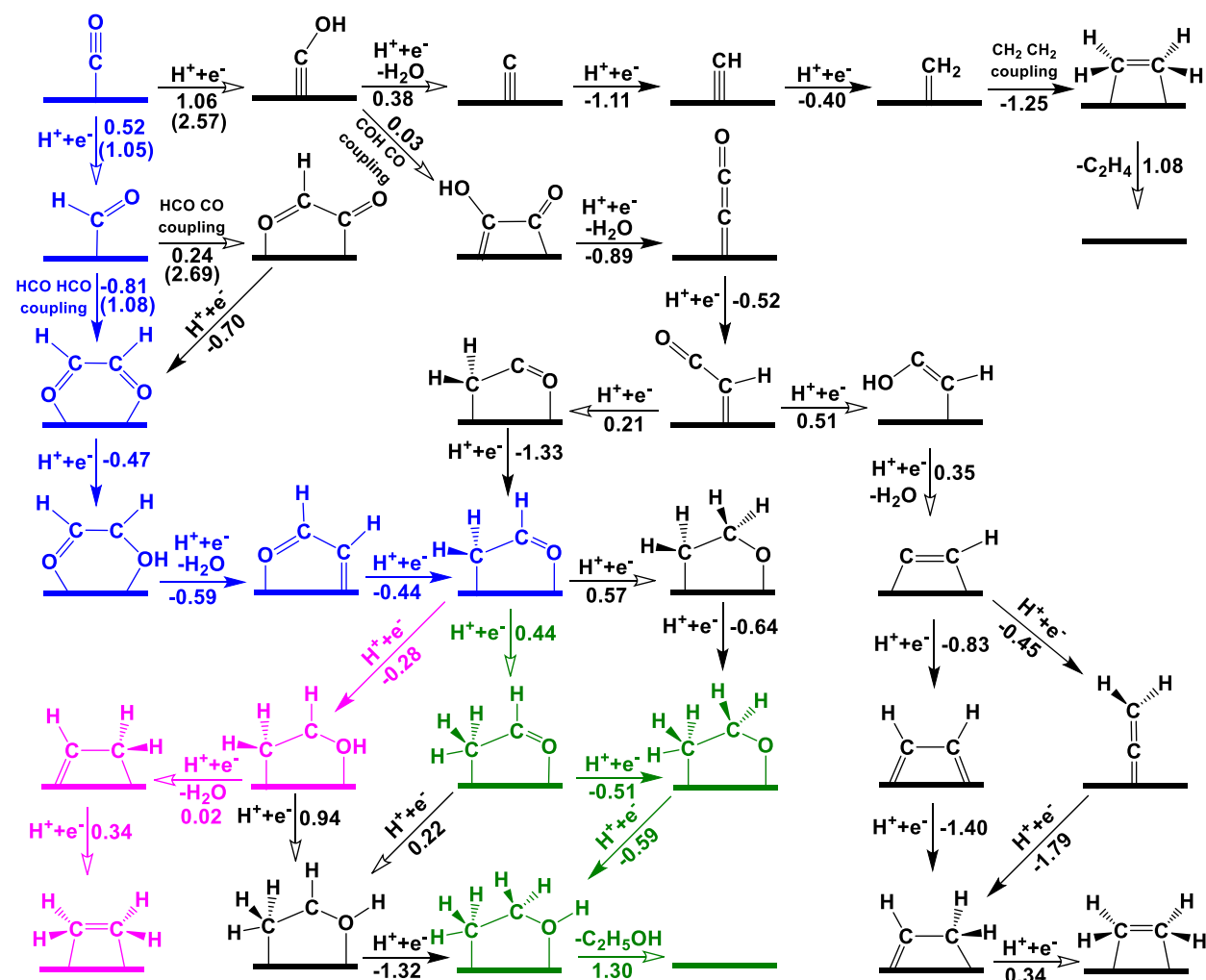
Scheme 2: All the possible mechanistic pathways with reaction free energies (in eV) for CO hydrogenation reaction to C_2H_4 and C_2H_5OH on Cu-dNC. The values given in the parenthesis are the activation barriers in eV at 0 V vs. RHE. The common intermediates of most favourable pathways are highlighted in blue color and the intermediates determine the selectivity of C_2H_4 and

C_2H_5OH are highlighted in magenta and green colors, respectively. The solid and hollow arrow heads represent the exergonic and endergonic steps, respectively.

3.4.2. Formation of C_2H_5OH: Along with C_2H_4 another important C_2 based CO_2 hydrogenated product is C_2H_5OH. Therefore, we have investigated the CO_2 hydrogenation to C_2H_5OH mechanistic pathways. There are some common intermediates for C_2H_5OH and C_2H_4 formations. The common intermediates of most favourable pathway for C_2H_4 formation are *CO, *HCO, *HCO-HCO, *HCO-HCOH, *HC-HCO, and *H_2C-HCO. In case of C_2H_5OH, the formation of *HCO-HCO is more favourable as it can be reduced to C_2H_5OH. The *HCO-HCO intermediate has also been identified for C_2H_5OH formation by several groups on periodic Cu(100) surfaces.[21,22] After identifying the common intermediates, possible pathways for C_2H_5OH formation have been investigated by calculating the reaction free energy of all the possible elementary step. The *H_2C-HCO can form C_2H_5OH via hydrogenation at three different positions and may form *H_2C-HCOH, *H_3C-HCO and *H_2C-H_2CO. The calculated reaction free energy values show that the hydrogenation step of *H_2C-HCO is exergonic if protonation occurs only at the O-center of the *H_2C-HCO. Then, further hydrogenation at the H_2C-center of *H_2C-HCOH and hydrogenation at the O-center of the *H_3C-HCO may form *H_3C-HCOH. Besides, hydrogenation at the HC-center of *H_3C-HCO and hydrogenation at the H_2C-center of *H_2C-H_2CO produce *H_3C-H_2CO with reaction free energies of -0.51 and -0.64 eV, respectively. In the next step, *H_3C-HCOH and *H_3C-H_2CO can be converted to *H_3C-H_2COH. Eventually, C_2H_5OH can be removed from the catalytic surface of Cu-dNC. This step is highly endergonic with a reaction free energy of 1.30 eV. Therefore, the amount of C_2H_5OH production is expected to be less. However, the most favourable pathway for CO_2 hydrogenation to C_2H_5OH is * + CO_2 → *CO_2 → *COOH → *CO → *HCO → *HCO-HCO → *HCO-HCOH → *HC-HCO → *H_2C-HCO → *H_3C-HCO → *H_3C-H_2CO →

*H₃C-H₂COH → * + C₂H₅OH with a total reaction free energy of -1.54 eV. Besides, *CO → *HCO is the PDS with a reaction free energy of 0.52 eV. Recently, Yeo and co-workers have shown C₂H₅OH pathway via *CH and *CO coupling on Cu(111) surface which are different than that of our favourable pathway on the Cu-dNC.[66] However, the *CO → *HCO has also been reported to be the PDS by several other studies on periodic Cu(100) surface but the required reaction free energy of the PDS step is higher in those studies than that on the Cu-dNC for C₂H₅OH formation.[21,22] Therefore, Cu-dNC can be an efficient catalyst for C₂H₅OH formation from CO₂.

4. Comparison among C₁ and C₂ based products

In this section, we have compared the C₁ and C₂ based products on the basis of working potential. The working potential is the minimum required potential at which all the elementary reaction steps become exergonic or reversible.[43] Hence, the required working potential is the potential of the most endergonic step i.e., PDS. In this case we have considered the most plausible mechanistic pathway for HCOOH, CH₃OH, CH₄, C₂H₄ and C₂H₅OH formation from CO₂. The relative reaction free energies and their dependencies on the applied potential are shown in Figure 5 and S5. Here, in case of HCOOH formation, *HCOOH from *HCOO is the most endergonic step with a reaction free energy of 0.55 eV. Hence, at -0.55 V all the steps of HCOOH formation will be thermodynamically favourable. Besides, for CH₃OH formation *CO → *HCO step is the most endergonic step and an amount of -0.52 V potential is required for CH₃OH formation. For CH₄, an amount of -1.06 V potential is required as *CO → *COH step is endergonic by 1.06 eV. Along with CH₃OH, *CO → *HCO is the most endergonic step for C₂H₄ and C₂H₅OH formation. Hence, at -0.52 V we can expect CH₃OH, C₂H₄ and C₂H₅OH on the Cu-dNC surface. Even if working potential is same for C₂H₅OH and C₂H₄, the calculated total reaction free energies show that

23

C_2H_5OH formation is 0.52 eV more favourable than that of C_2H_4 on the Cu-dNC surface. Hence, the amount of C_2H_5OH formation will be more compared to C_2H_4 on the Cu-dNC. Earlier reports suggest that *CO to *HCO is the potential limiting step on the Cu_{85} nanocluster and periodic Cu(111) surface with required potential of -0.53 and -0.71 V respectively for CH_3OH formation.[57,63]
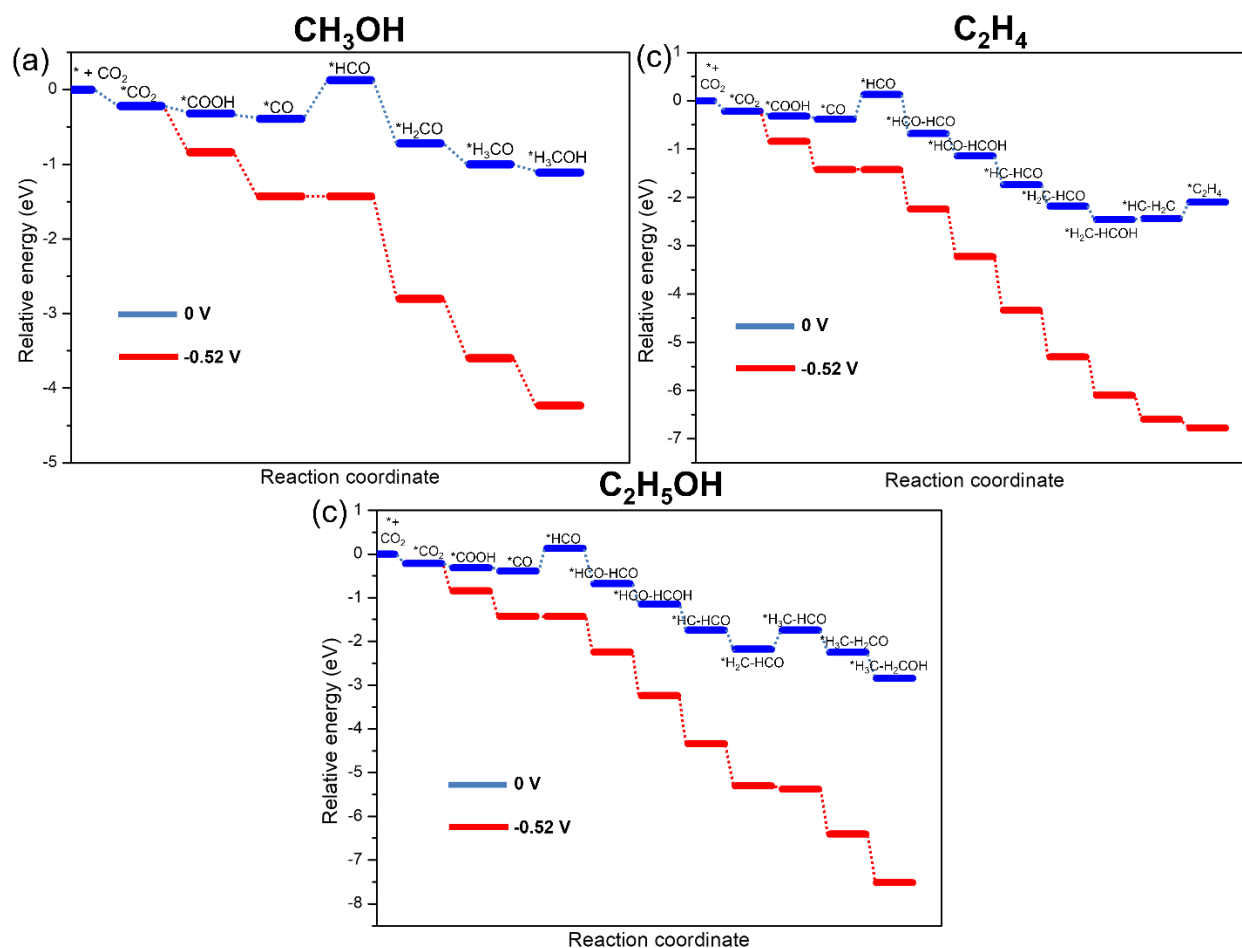

Figure 5: Reaction free energies of CO_2 hydrogenation to CH_3OH, C_2H_4 and C_2H_5OH and their dependencies on the applied potentials.

Moreover, earlier reports have reported the most endergonic step with 0.62 and 0.65 eV on the periodic Cu(100) surface for C_2 based product formation from CO_2.[21,22] Thus, Cu-dNC can be

considered as an efficient and promising catalyst for CO_2 hydrogenation reaction to C_2 based product formation. To understand the reason behind the superior catalytic activity of the Cu(100) facet of the Cu-dNC compared to the periodic Cu(100) surface, we have investigated the d-band-center energies. The calculated d-band-center energies are -2.45 and -2.43 eV for periodic Cu(100) surface and Cu(100) facet, respectively. Therefore, the calculated d-band-center energies of the Cu(100) and Cu(100) facet are more or less same. The Cu-Cu bond distances are 2.47 Å on the periodic Cu(100) surface whereas the Cu-Cu average bond distance is 2.52 Å as various Cu-Cu bond lengths are observed (2.56, 2.76, 2.42 and 2.35 Å) on the Cu-dNC surface. So, Cu-dNC is highly distorted compared to the periodic Cu(100) surface. Our calculated strain value shows that Cu-dNC is under tensile strain (10.99%) compared to the periodic Cu(100) surface. Therefore, the formation of *HCO from *CO is favourable on the Cu-dNC as distorted surface can stabilize the intermediates as also reported by Rojas and co-workers, who have shown that the lattice distortion of the catalyst can influence the activity, higher distortion results higher catalytic activity.[67]

5. Conclusion

We have used DFT studies for the investigation of the most favourable pathways of CO_2 hydrogenation to various C_1 and C_2 based products on the Cu(100) facet of a Cu-NC based nanocluster At first, the stability of the modelled Cu-NC has been examined and we have found out that the formation of the Cu-NC is energetically favorable though the structure is not dynamically and thermally stable as the structure converts to a minimum energy structure at higher temperatures. The structure distorts to another structure (Cu-dNC) which is calculated to be stable. Hence, the CO_2 hydrogenation reaction to C_1 and C_2 based products has been studied on the Cu-dNC catalyst. Our calculated adsorption energies and mechanistic pathways explains various

important observations including the reason behind the superior activity of Cu-dNC for product selectivity towards C_2 based products. We find that that most of the considered intermediates adsorb strongly on the Cu-dNC compared to that on the periodic Cu(111) surface. The trend in adsorption energies of the intermediate can be explained using the PDOS and Bader charge analysis. We have also studied the effect of applied potential on the product formation steps and the calculated results indicate that the formation of CH_3OH, C_2H_4 and C_2H_5OH are favourable at -0.52 V. On the other hand, our calculated reaction energy values (-0.38 eV for CH_3OH, -1.02 eV for C_2H_4, and -1.54 eV C_2H_5OH) show that the formation of C_2 based products are highly exergonic compared to C_1 (methanol) formation. Hence, Cu-dNC can be considered as efficient catalyst for the C_2 based products compared to that on the periodic Cu(100) surface. This may be due to the distorted surface of Cu-dNC which stabilize the intermediates responsible for C_2 based products formation. To the best of our knowledge, this is the first theoretical reports of CO_2 hydrogenation reaction for various C_1 and C_2 based product formation on a Cu-NC based model. We believe that these finding will be helpful for theorists as well as experimentalists working on the CO_2 hydrogenation reaction for the designing of efficient and selective catalyst.

Associated content

Supporting Information: Snapshots of the Cu-NC and Cu-dNC at the end of the AIMD simulations, adsorption patterns of the considered C_1 and C_2 based intermediates, relative reaction free energies and dependencies on the applied potential of CO_2 hydrogenation to HCOOH and CH_4.

Conflicts of interest

There are no conflicts to declare.

Acknowledgments

References

(1) Olah, G. A.; Prakash, G. K. S.; Goeppert, A. Anthropogenic Chemical Carbon Cycle for a Sustainable Future. *J. Am. Chem. Soc.* **2011**, *133*, 12881−12898.

(2) Ghadimkhani, G.; Tacconi, N. R. de; Chanmanee, W.; Janaky, C.; Rajeshwar, K. Efficient solar photoelectrosynthesis of methanol from carbon dioxide using hybrid CuO–Cu$_2$O semiconductor nanorod arrays. *Chem. Commun.* **2013**, *49*, 1297−1299.

(3)   Yin, L.; Liebscher, J. Carbon−Carbon Coupling Reactions Catalyzed by Heterogeneous Palladium Catalysts. *Chem. Rev.* **2007**, *107*, 133−173.

(4)   Hori, Y. In Modern Aspects of Electrochemistry, Vayenas, C. G.; White, R. E.; Gamboa-Aldeco, M. E. Eds.; Springer: New York, **2008**; Vol. *42*, pp 89−189.

(5)   Sapountzi, F. M.; Gracia, J. M.; Weststrate, C. J.; Fredriksson, H. O. A.; Niemantsverdriet, J. W. Electrocatalysts for the generation of hydrogen, oxygen and synthesis gas. *Prog. Energy Combust. Sci.* **2017**, *58*, 1-35.

(6)   Luo, W.; Zhang, J.; Li, M.; Züttel, A. Boosting CO Production in Electrocatalytic CO_2 Reduction on Highly Porous Zn Catalysts. *ACS Catal.* **2019**, *9,* 3783−3791.

(7)   Lamaison, S.; Wakerley, D.; Blanchard, J.; Montero, D.; Rousse, G.; Mercier, D.; Marcus, P.; Taverna, D.; Giaume, D.; Mougel, V.; Fontecave, M. High-Current-Density CO_2-to-CO Electroreduction on Ag-Alloyed Zn Dendrites at Elevated Pressure. *Joule* **2020**, *4*, 395–406.

(8)   Sun, R.; Liao, Y.; Bai, S.-T.; Zheng, M.; Zhou, C.; Zhang, T.; Sels, B. F. Heterogeneous catalysts for CO_2 hydrogenation to formic acid/formate: from nanoscale to single atom. *Energy Environ. Sci.* **2021**, *14*, 1247–1285.

(9)   Gunasekar, G. H.; Park, K.; Jung, K.-D.; Yoon, S. Recent developments in the catalytic hydrogenation of CO_2 to formic acid/formate using heterogeneous catalysts. *Inorg. Chem. Front.* **2016**, *3,* 882–895.

(10) Hori, Y.; Kikuchi, K.; Suzuki, S. Production of CO and CH_4 in Electrochemical Reduction of CO_2 at Metal Electrodes in Aqueous Hydrogencarbonate Solution. *Chem. Lett.* **1985**, *14*, 1695−1698.

(11) Hori, Y.; Kikuchi, K.; Murata, A.; Suzuki, S. Production of Methane and Ethylene in Electrochemical Reduction of Carbon Dioxide at Copper Electrode in Aqueous Hydrogencarbonate Solution. *Chem. Lett.* **1986**, *15*, 897−898.

(12) Hori, Y.; Murata, A.; Takahashi, R. J. Formation of hydrocarbons in the electrochemical reduction of carbon dioxide at a copper electrode in aqueous solution. *Chem. Soc., Faraday Trans. 1* **1989**, *85*, 2309−2326.

(13) Hori, Y.; Wakebe, H.; Tsukamoto, T.; Koga, O. Adsorption of CO accompanied with simultaneous charge transfer on copper single crystal electrodes related with electrochemical reduction of CO_2 to hydrocarbons. *Surf. Sci.* **1995**, *335*, 258−263.

(14) Takahashi, I.; Koga, O.; Hoshi, N.; Hori, Y. Electrochemical reduction of CO_2 at copper single crystal Cu(S)-[n(111)×(111)] and Cu(S)-[n(110)×(100)] electrodes. *J. Electroanal. Chem.* **2002**, *533*, 135−143.

(15) Hori, Y.; Takahashi, I.; Koga, O.; Hoshi, N. Electrochemical reduction of carbon dioxide at various series of copper single crystal electrodes. *J. Mol. Catal. A: Chem.* **2003**, *199*, 39−47.

(16) Schouten, K. J. P.; Kwon, Y.; van der Ham, C. J. M.; Qin, Z.; Koper, M. T. M. A new mechanism for the selectivity to C_1 and C_2 species in the electrochemical reduction of carbon dioxide on copper electrodes. *Chem. Sci.* **2011**, *2*, 1902−1909.

(17) Schouten, K. J. P.; Qin, Z. S.; Gallent, E. P.; Koper, M. T. M. Two Pathways for the Formation of Ethylene in CO Reduction on Single-Crystal Copper Electrodes. *J. Am. Chem. Soc.* **2012**, *134*, 9864−9867.

(18) Kortlever, R.; Shen, J.; Schouten, K. J. P.; Calle-Vallejo, F.; Koper, M. T. M. Catalysts and Reaction Pathways for the Electrochemical Reduction of Carbon Dioxide. *J. Phys. Chem. Lett.* **2015**, *6*, 4073−4082.

(19) Calle-Vallejo, F.; Koper, M. T. M. Theoretical Considerations on the Electroreduction of CO to C_2 Species on Cu(100) Electrodes. *Angew. Chem.* **2013**, *125*, 7423−7426.

(20) Montoya, J. H.; Shi, C.; Chan, K.; Nørskov, J. K. Theoretical Insights into a CO Dimerization Mechanism in CO_2 Electroreduction. *J. Phys. Chem. Lett.* **2015**, *6*, 2032−2037.

(21) Luo, W.; Nie, X.; Janik, M. J.; Asthagiri, A. Facet Dependence of CO_2 Reduction Paths on Cu Electrodes. *ACS Catal.* **2016**, *6*, 219−229.

(22) Garza, A. J.; Bell, A. T.; Head-Gordon, M. Mechanism of CO_2 Reduction at Copper Surfaces: Pathways to C_2 Products. *ACS Catal.* **2018**, *8*, 1490−1499.

(23) Mangione, G.; Huang, J.; Buonsanti, R.; Corminboeuf, C. Dual-Facet Mechanism in Copper Nanocubes for Electrochemical CO_2 Reduction into Ethylene. *J. Phys. Chem. Lett.* **2019**, *10*, 4259−4265.

(24) Gregorio, G. L. D.; Burdyny, T.; Loiudice, A.; Iyengar, P.; Smith, W. A.; Buonsanti, R. Facet-Dependent Selectivity of Cu Catalysts in Electrochemical CO_2 Reduction at Commercially Viable Current Densities. *ACS Catal.* **2020**, *10*, 4854−4862.

(25) Todorova, T. K.; Schreiber, M. W.; Fontecave, M. Mechanistic Understanding of CO_2 Reduction Reaction (CO_2RR) Toward Multicarbon Products by Heterogeneous Copper-Based Catalysts. *ACS Catal.* **2020**, *10*, 1754−1768.

(26) Roberts, F. S.; Kuhl, K. P.; Nilsson, A. High Selectivity for Ethylene from Carbon Dioxide Reduction over Copper Nanocube Electrocatalysts. *Angew. Chem. Int. Ed.* **2015**, *54*, 5179 −5182.

(27) Baruch, M. F.; Pander, J. E.; White, J. L.; Bocarsly, A. B. Mechanistic Insights into the Reduction of CO2 on Tin Electrodes using in Situ ATR-IR Spectroscopy. *ACS Catal.* **2015**, *5*, 3148−3156.

(28) Figueiredo, M. C.; Ledezma-Yanez, I.; Koper, M. T. M. In Situ Spectroscopic Study of CO_2 Electroreduction at Copper Electrodes in Acetonitrile. *ACS Catal.* **2016**, *6*, 2382−2392.

(29) Bagger, A.; Ju, W.; Varela, A. S.; Strasser, P.; Rossmeisl, J. Electrochemical CO_2 Reduction: A Classification Problem. *ChemPhysChem* **2017**, *18*, 3266–3273.

(30) Lin, Z.; Zhong, S.; Grierson, D. Recent advances in ethylene research. *J. Exp. Bot.* **2009**, *60*, 3311–3336.

(31) Goldemberg, J. Ethanol for a Sustainable Energy Future. *Science* **2007**, *315*, 808-810.

(32) Badwal, S. P. S.; Giddey, S.; Kulkarni, A.; Goel, J.; Basu, S. Direct ethanol fuel cells for transport and stationary applications – A comprehensive review. *Appl. Energy* **2015**, *145*, 80−103.

(33) Wang, W.; Wang, S.; Ma, X.; Gong, J. Recent advances in catalytichydrogenation of carbon dioxide. *Chem. Soc. Rev.* **2011**, *40*, 3703–3727.

(34) Fukuzumi, S. Production of Liquid Solar Fuels and Their Use in Fuel Cells. *Joule* **2017**, *1*, 689–738.

(35) Blöchl, P. E. Projector augmented-wave method. *Phys. Rev. B: Condens. Matter Mater. Phys.* **1994**, *50*, 17953–17979.

(36) Kresse, G.; Joubert, D. From ultrasoft pseudopotentials to the projector augmented-wave method. *Phys. Rev. B: Condens. Matter Mater. Phys.* **1999**, *59*, 1758–1775.

(37) Kresse, G.; Furthmüller, J. Efficient iterative schemes for ab initio total-energy calculations using a plane-wave basis set. *Phys. Rev. B: Condens. Matter Mater. Phys.* **1996**, *54*, 11169–11186.

(38) Perdew, J. P.; Burke, K.; Ernzerhof, M. Generalized Gradient Approximation Made Simple. *Phys. Rev. Lett.* **1996**, *77*, 3865–3868.

(39) Perdew, J. P.; Burke, K.; Ernzerhof, M. Generalized Gradient Approximation Made Simple [Phys. Rev. Lett. 77, 3865 (1996)]. *Phys. Rev. Lett.* **1997**, *78*, 1396.

(40) Perdew, J. P.; Chevary, J. A.; Vosko, S. H.; Jackson, K. A.; Pederson, M. R.; Singh, D. J.; Fiolhais, C. Atoms, molecules, solids, and surfaces: Applications of the generalized gradient approximation for exchange and correlation. *Phys. Rev. B: Condens. Matter Mater. Phys.* **1992**, *46*, 6671−6687.

(41) Grimme, S.; Antony, J.; Ehrlich, S.; Krieg, H. A consistent and accurate ab initio parametrization of density functional dispersion correction (DFT-D) for the 94 elements H-Pu. *J. Chem. Phys.* **2010**, *132*, 154104.

(42) Nørskov, J. K.; Rossmeisl, J.; Logadottir, A.; Lindqvist, L.; Kitchin, J. R.; Bligaard, T.; Jonsson, H. Origin of the Overpotential for Oxygen Reduction at a Fuel-Cell Cathode. *J. Phys. Chem. B* **2004**, *108*, 17886–17892.

(43) Karamad, M.; Hansen, H. A.; Rossmeisl, J.; Nørskov, J. K. Mechanistic Pathway in the Electrochemical Reduction of CO_2 on RuO_2. *ACS Catal.* **2015**, *5*, 4075–4081.

(44) Peterson, A. A.; Abild-Pedersen, F.; Studt, F.; Rossmeisl, J.; Nørskov, J. K. How copper catalyzes the electroreduction of carbon dioxide into hydrocarbon fuels. *Energy Environ. Sci.* **2010**, *3*, 1311–1315.

(45) Henkelman, G.; Uberuaga, B. P.; Jónsson, H. A climbing image nudged elastic band method for finding saddle points and minimum energy paths. *J. Chem. Phys.* **2000**, *113*, 9901−9904.

(46) Henkelman, G.; Jónsson, H. A dimer method for finding saddle points on high dimensional potential surfaces using only first derivatives. *J. Chem. Phys.* **1999**, *111*, 7010−7022.

(47) Tang, W.; Sanville, E.; Henkelman, G. A grid-based Bader analysis algorithm without lattice bias. *J. Phys.: Condens. Matter* **2009**, *21*, 084204.

(48) Sanville, E.; Kenny, S. D.; Smith, R.; Henkelman, G. Improved grid-based algorithm for Bader charge allocation. *J. Comput. Chem.* **2007**, *28*, 899–908.

(49) Henkelman, G.; Arnaldsson, A.; Jónsson, H. A fast and robust algorithm for Bader decomposition of charge density. *Comput. Mater. Sci.* **2006**, *36*, 354-360.

(50) Shi, Z.; Zhang, Z.; Kutana, A.; Yakobson, B. I. Predicting Two-Dimensional Silicon Carbide Monolayers. *ACS Nano* **2015**, *9*, 9802−9809.

(51) Garg, P.; Kumar, S.; Choudhuri, I.; Mahata, A.; Pathak, B. Hexagonal Planar CdS Monolayer Sheet for Visible Light Photocatalysis. *J. Phys. Chem. C* **2016**, *120*, 7052−7060.

(52) Feibelman, P. J. First-principles step- and kink-formation energies on Cu(111). *Phys. Rev. B: Condens. Matter Mater. Phys.* **1999**, *60*, 11118−11122.

(53) Zhang, Z.; Liu, X.; Yakobson, B. I.; Guo, W. Two-Dimensional Tetragonal TiC Monolayer Sheet and Nanoribbons. *J. Am. Chem. Soc.* **2012**, *134*, 19326−19329.

(54) Zhou, J.; Huang, J.; Sumpter, B. G.; Kent, P. R. C.; Xie, Y.; Terrones, H.; Smith, S. C. Theoretical Predictions of Freestanding Honeycomb Sheets of Cadmium Chalcogenides. *J. Phys. Chem. C* **2014**, *118*, 16236−16245.

(55) Waugh, K. C. Methanol Synthesis. *Catal. Today* **1992**, *15*, 51–75.

(56) Nosé, S. A unified formulation of the constant temperature molecular dynamics methods. *J. Chem. Phys.* **1984**, *81*, 511–519.

(57) Rawat, K. S.; Mahata, A.; Pathak, B. Thermochemical and electrochemical CO_2 reduction on octahedral Cu nanocluster: Role of solvent towards product selectivity. *J. Catal.* **2017**, *349*, 118–127.

(58) Muttaqien, F.; Hamamoto, Y.; Inagaki, K.; Morikawa, Y. Dissociative adsorption of CO_2 on flat, stepped, and kinked Cu surfaces. *J. Chem. Phys.* **2014**, *141*, 034702.

(59) Grabow, L. C.; Mavrikakis, M. Mechanism of Methanol Synthesis on Cu through CO_2 and CO Hydrogenation. *ACS Catal.* **2011**, *1*, 365–384.

(60) Zhang, X.; Liu, J.-X.; Zijlstra, B.; Filot, I. A. W.; Zhou, Z.; Sun, S.; Hensen, E. J. M. Optimum Cu nanoparticle catalysts for CO_2 hydrogenation towards methanol. *Nano Energy* **2018**, *43*, 200−209.

(61) Mandal, S. C.; Pathak, B. Computational insights into selective CO_2 hydrogenation to CH_3OH catalysed by ZnO based nanocages. *Mater. Adv.* **2020**, *1*, 2300-2309.

(62) Mandal, S. C.; Rawat, K. S.; Garg, P.; Pathak, B. Hexagonal Cu(111) Monolayers for Selective CO_2 Hydrogenation to CH3OH: Insights from Density Functional Theory. *ACS Appl. Nano Mater.* **2019**, *2*, 7686−7695.

(63) Nie, X.; Luo, W.; Janik, M. J.; Asthagiri, A. Reaction mechanisms of CO_2 electrochemical reduction on Cu(111) determined with density functional theory. *J. Catal.* **2014**, *312*, 108-122.

(64) Hori, Y.; Takahashi, R.; Yoshinami, Y.; Murata, A. Electrochemical Reduction of CO at a Copper Electrode. *J. Phys. Chem. B* **1997**, *101*, 7075-7081.

(65) Ma, W.; Xie, S.; Liu, T.; Fan, Q.; Ye, J.; Sun, F.; Jiang, Z.; Zhang, Q.; Cheng, J.; Wang, Y. Electrocatalytic reduction of CO_2 to ethylene and ethanol through hydrogen-assisted C–C coupling over fluorine-modified copper. *Nat. Catal*. **2020**, *3*, 478–487.

(66) Ting, L. R. L.; Piqué, O.; Lim, S. Y.; Tanhaei, M.; Calle-Vallejo, F.; Yeo, B. S. Enhancing CO_2 Electroreduction to Ethanol on Copper–Silver Composites by Opening an Alternative Catalytic Pathway. *ACS Catal.* **2020**, *10*, 4059−4069.

(67) Retuerto, M.; Pascual, L.; Pique, O.; Kayser, P.; Salam, M. A.; Mokhtar, M.; Alonso, J. A.; Pena, M.; Calle-Vallejo, F.; Rojas, S. How oxidation state and lattice distortion influence the oxygen evolution activity in acid of iridium double perovskites. *J. Mater. Chem. A* **2021**, *9*, 2980–2990.

Table of Contents